First-Principles Study on Electronic Structures of $FAPbX_3$ (X = Cl, Br, I) Hybrid Perovskites

Y. Y. Pan[1,2] , Y. H. Su[1*], C. H. Hsu[2] , L. W. Huang[1,2] , K. P. Dou[2] and C. C. Kaun[2*]

[1] Department of Materials Science and Engineering, National Cheng Kung University, Tainan, Taiwan
[2] Research Center for Applied Sciences, Academia Sinica, Taipei, Taiwan
Email: yhsu@mail.ncku.edu.tw, kauncc@gate.sinica.edu.tw

Abstract. Using first principles calculations, we investigate the geometric and electronic structures of organic–inorganic hybrid perovskite, $FAPbX_3$ ($FA = CH(NH_2)_2^+$; X = Cl, Br, I). Since the organic molecule in the centre of the 3D hybrid perovskite is the key for its characteristics, here we compare $FAPbX_3$ with $MAPbX_3$ ($MA = CH_3NH_3^+$). The band gap of the former is smaller than the latter. Particularly, the calculated band gap of $FAPbI_3$, 1.40 eV, is close to the experimental data, 1.41 eV. Furthermore, we analyze their orbitals, density of states and the spatial distribution of the charges, revealing that $FAPbX_3$ can produce and transfer more excitons than $MAPbX_3$ does.

Keywords: Solar cell, formamidinium, methylammonium, geometric structure, band gap.

1 Introduction

Perovskite solar cells (PSCs) have been the most promising devices towards the renewable energy generation recently, whose highest efficiency, 21.1%, was achieved in 2016 [1]. In addition to their efficient light absorption and high carrier mobility [2-4], they are semiconductors with adjustable band gaps, which have the benefits to absorb different wavelengths of light [5] and to fit into the solar devices well [6]. However, the performance of perovskite depends on its structural order which is temperature-dependent even in typical solar cell operating conditions. For example, methylammonium (MA, $CH_3NH_3^+$) lead iodide (PbI_3) undergoes a phase transition between tetragonal and cubic symmetry within 54 and 57 °C [7, 8]. Increasing the temperature increases the kinetic energy of the organic molecule in the perovskite [9, 10] and creates volatile molecular defects towards the structure degradation [11]. These factors affect the PSC durability.

Improving the perovskite stability thus is the key issue for solar cells, and formamidinium (FA, $CH(NH_2)_2^+$) cations were recently suggested, by plane-wave first-principles calculations, to replace MA inside the inorganic metrix [12, 13], due to that the former can interact with the inorganic cage stronger than the latter does, to reduce the release of volatile species [13] or alter the covalent/ionic character of Pb-I bonds [12]. On the other hand, mixing FA with MA is experimentally shown to be a route to stabilize the perovskite [8, 14] and improve the power conversion efficiency [14]. However, first-principles calculations with the linear combination of atomic orbital (LCAO) basis-set, which are economical and feasible for charge transport studies, on this issue are still limited to date.

In this work, we investigate the geometric and electronic properties of organic-inorganic hybrid perovskite, $FAPbX_3$ (X = Cl, Br, I) from first principles. Particularly, their geometries, band structures, orbitals, density of states, and the charge densities are analysed, revealing the electronic and optical properties, as well as the stability, of such materials. In addition, we compare the band gap of $FAPbI_3$ with the measured data. Finally, we compare the electronic features of $FAPbX_3$ with $MAPbX_3$.

2 Computational Methods

The structural optimization was done by using Siesta, a density functional theory based code, with self-consistent field method. The conjugate gradient method was used for optimization, with the local density approximation and the LCAO basis-set. The optimized structures were then used to calculate the electronic structures by the density functional theory and the non-equilibrium Green function

formalism based code, Nanodcal. The calculated $FAPbX_3$ are simple cubic. The lattice constants of $FAPbCl_3$, $FAPbBr_3$ and $FAPbI_3$ are 5.61567, 5.7688 and 6.3992 Å, respectively, within ±40% of the optimized lattice constants of $MAPbCl_3$, $MAPbBr_3$ and $MAPbI_3$ (5.675, 5.901 and 6.329 Å, respectively [15]). The K-points set was 20x20x20. The Brillouin zone went along two paths: RGXMG and XRMRG. The density of states and charge density were projected on s, p, d orbitals of all atoms.

3 Results and Discussion

Figure 1 shows the initial and optimized cubic structures of $FAPbCl_3$, $FAPbBr_3$ and $FAPbI_3$. The inorganic frames of the perovskites are distorted. The N-C-N bond of the FA molecule transforms from lying on (001) plane to (110) plane which is the most stable site for FA inside the PbX_3 frame. Figure 2 plots the brillouin zone of the cubic structure [16]. To cover all the K points, it must draw from Gamma point (G), to M, R, G, X, M, G, R, X points.

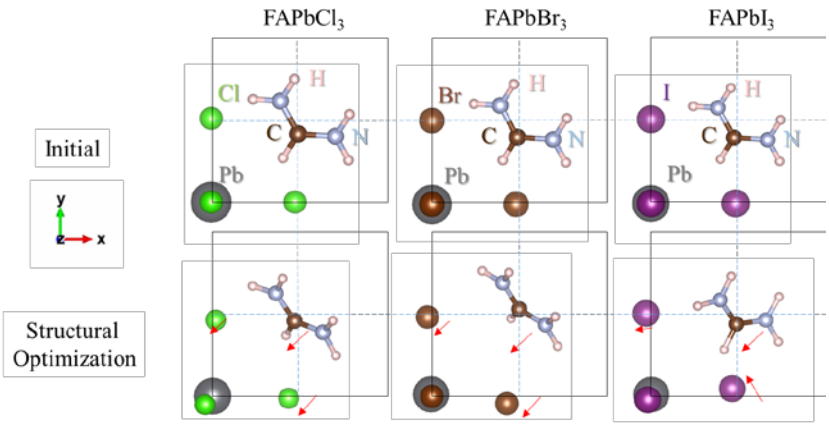

Figure 1. Structural optimization of $FAPbX_3$ (X= Cl, Br and I)

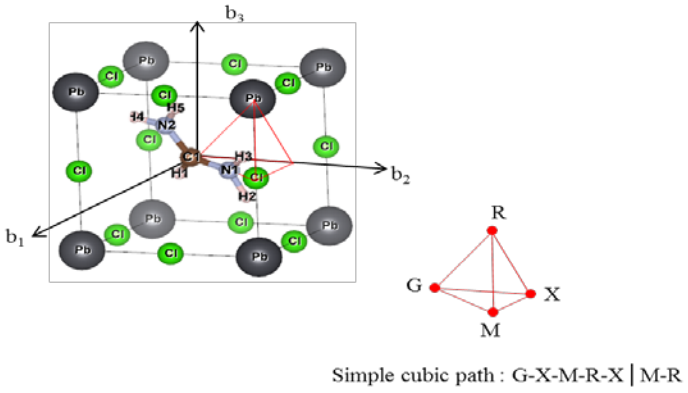

Figure 2. The brillouin zone of a simple cubic lattice.

In Figure 3, the band structures of $FAPbX_3$ indicate that the band gaps locate at the R point with the values of 2.02, 1.65 and 1.40 eV for $FAPbCl_3$, $FAPbBr_3$ and $FAPbI_3$, respectively. They are direct band gaps, checked with the M-R point path. Our calculated band gap of $FAPbI_3$ ($FAPbBr_3$) is about 0.01 (0.50) eV smaller than the measured value 1.41 (2.15) eV [17] or 1.47 eV [18]. To open up the band gap, the relativistic GW calculations may be needed [19, 20].

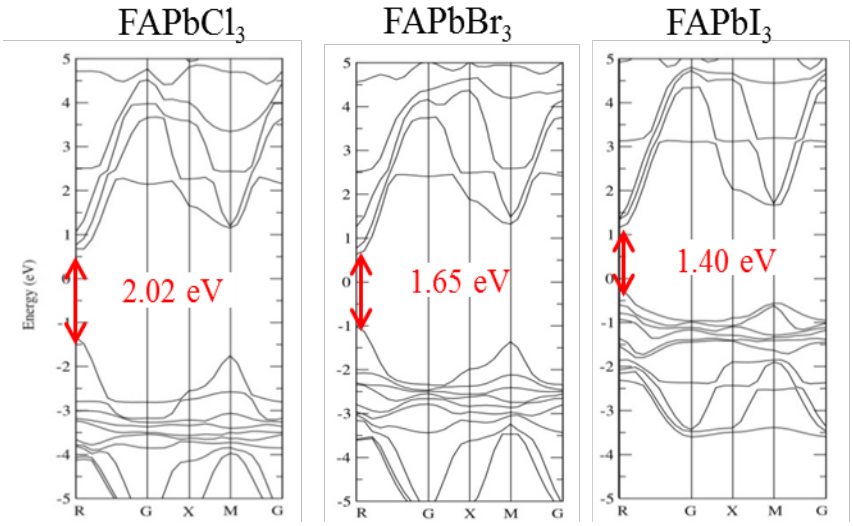

Figure 3. E-k diagram of $FAPbX_3$ (Path: R-G-X-M-G)

Whereas the band gaps of $FAPbX_3$ depend on their geometries and configurations, the band structures near the Fermi level are similar. The band structures shown in Figure 3 thus are used as examples to investigate the orbitals consisting of the conduction and valence bands around the Fermi level. The larger the contribution of the orbital does, the bigger the circle on the band structure is. Figure 4 shows that the p orbital of the Pb atom affects the conduction band minimum, while the s and p orbitals of the X (Cl, Br and I) atoms influence the valence band maximum. The band structures of $FAPbX_3$ (Fig. 4 a-c) are similar with those of $MAPbX_3$ (Fig. 4 d-f) [21]. However, the s orbitals of Cl and Br atoms in $MAPbX_3$ (Fig. 4d and 4e) does not influence the valence band maximum, rather than in $FAPbX_3$ cases (Fig. 4a and 4b).

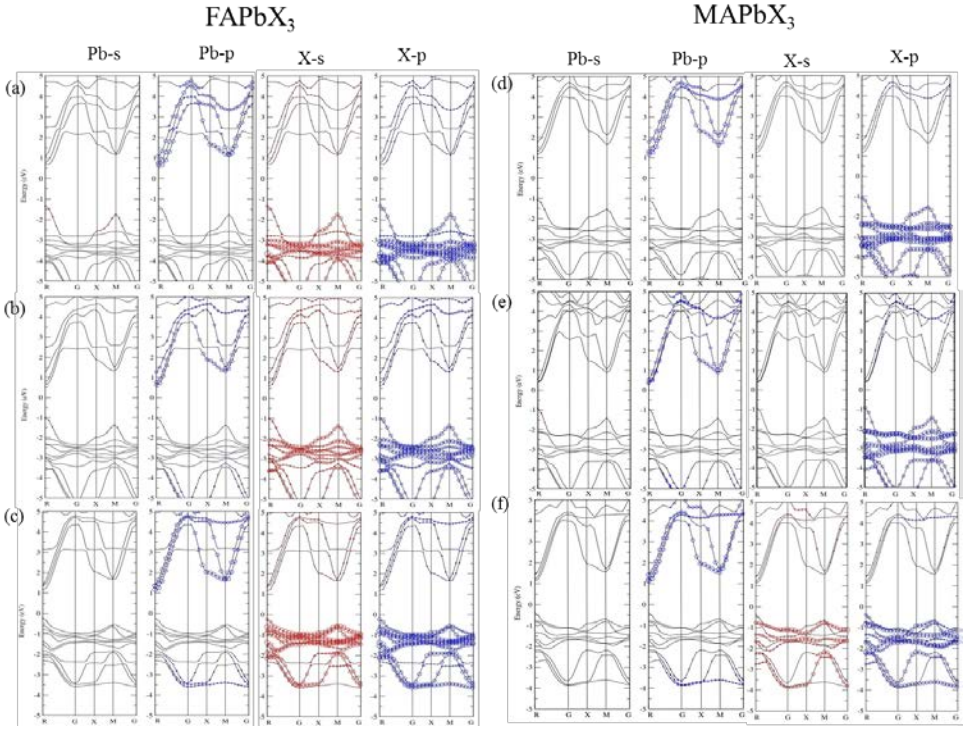

Figure 4. The contribution of the s and p orbitals of Pb and X atoms projected on the band structures of (a) $FAPbCl_3$, (b) $FAPbBr_3$, (c) $FAPbI_3$, (d) $MAPbCl_3$, (e) $MAPbBr_3$ and (f) $MAPbI_3$.

In Figure 5, each top panel shows the total density of states and the following panels plot the partial density of states of the Pb atom, the halogen atoms, and the organic cations (FA or MA) for $FAPbCl_3$ (a), $FAPbBr_3$ (b), $FAPbI_3$ (c), $MAPbCl_3$ (c), $MAPbBr_3$ (d) and $MAPbI_3$ (e), respectively. The p orbital of the Pb atom governs the conduction band, while the p orbitals of the halogen atoms constituent the valence band. In addition, the s orbital of I atom also contributes to the valence band. Thus the valence band maximum of $FAPbI_3$ is closer to the Fermi energy (at around 0.5 eV) and has larger density of states than those of other $FAPbX_3$. Moreover, the valence band maximum of $FAPbI_3$ is also closer to the Fermi energy than that of $MAPbI_3$, giving a smaller band gap. The former also has higher density of states around the valence band maximum than the latter, due to the contribution of s and p orbitals of I atoms, induced by the FA cations. Therefore, $FAPbI_3$ has more states for occupation. As this material is photo excited, more excitons can be produced, which are also easier transferred than other organic-inorganic hybrid perovskite.

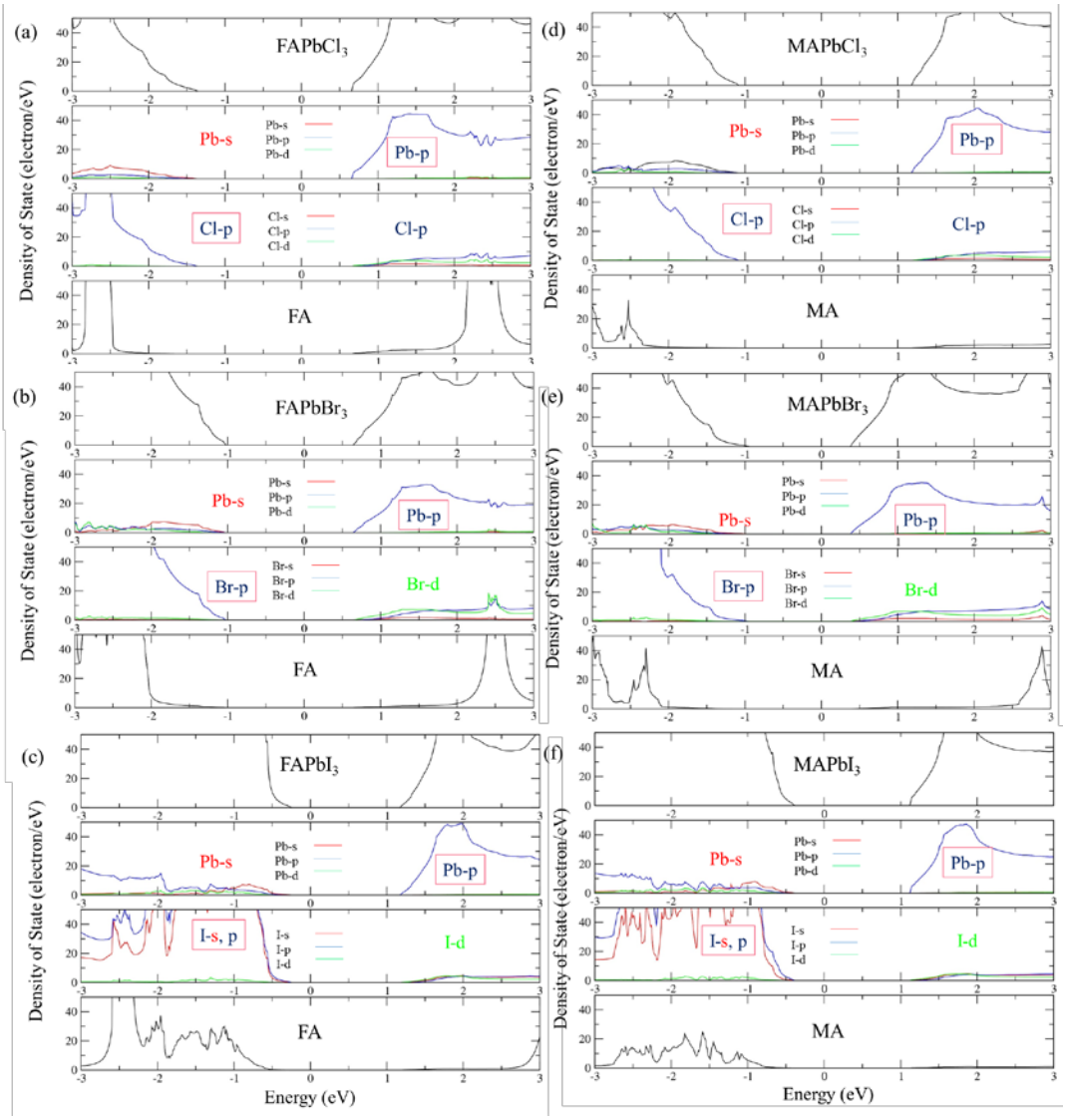

Figure 5. Density of states of (a) $FAPbCl_3$, (b) $FAPbBr_3$, (c) $FAPbI_3$, (d) $MAPbCl_3$, (e) $MAPbBr_3$ and (f) $MAPbI_3$.

Figure 6 shows the charge distribution in real space. The energy range of the conduction band charge density is between 0 to 40 eV, shown in Figure 6a (6c), where the isosurface of FA (MA) molecule is bigger because it is positive ions. The energy range of the valence band charge density is between -40 to 0 eV, shown in Figure 6b (6d), where the isosurface of PbX_3^- is bigger because Pb and X are negative

ions. In Figure 6a (6c), the order of conduction band molecular charge density from the big to the small is $APbCl_3$, $APbBr_3$ and $APbI_3$, following the order of electronegativity in chlorine, bromine and iodine. The higher electronegativity it is, then the more ionization it has. However, the charge distribution of FA cations are larger than MA ones, supporting that FA cations interact with the Pb-X frame stronger than MA, making the systems more stable.

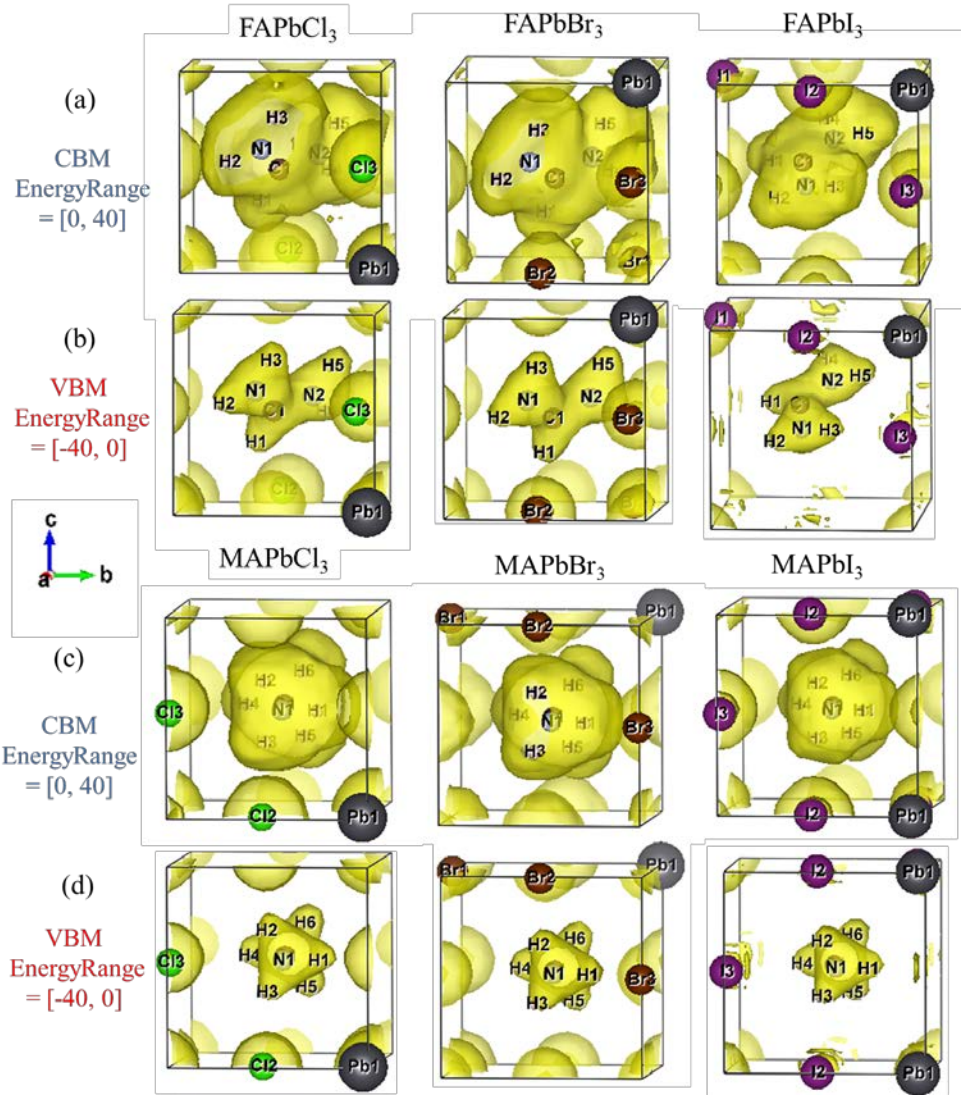

Figure 6. Charge densities in real space of (a) $FAPbCl_3$, (b) $FAPbBr_3$, (c) $FAPbI_3$, (d) $MAPbCl_3$, (e) $MAPbBr_3$ and (f) $MAPbI_3$.

4 Conclusion

In summary, we have investigated the geometric and electronic structures of $FAPbX_3$ (X = Cl, Br, I) from first principles. The calculated band gap of $FAPbI_3$, 1.40 eV, is close to the experimental data, 1.41 eV [17] or 1.47 eV [18]. The band gap of $FAPbI_3$ (1.40 eV) are smaller than the band gap of $MAPbI_3$ (1.52 eV) [21], so that $FAPbI_3$ has broader light absorption than conventional $MAPbI_3$. While the band gaps of $FAPbX_3$ and $MAPbX_3$ are different, their band structures are similar. However, around the valence band maximum, $FAPbI_3$ have higher density of states than $MAPbI_3$, suggesting that the organic molecule (FA or MA) can tune the electronic properties of the perovskite. The charge distribution of FA molecule is larger than MA molecule, supporting that FA molecule make the Pb-X framework more

stable. Our results indicate that $FAPbX_3$ could be used to build a better perovskite solar cell than $MAPbX_3$ is, improving its efficiency and durability.

References

1. M. Saliba, T. Matsui, J. Y. Seo, K. Domanski, J. P. Correa-Baena, M. K. Nazeeruddin, and M. Grätzel, "Cesium-containing triple cation perovskite solar cells: improved stability, reproducibility and high efficiency," *Energy & Environmental Science*, vol. 9, pp.1989-1997, 2016.
2. A. Kojima, M. Ikegami, K. Teshima, and T. Miyasaka, "Highly luminescent lead bromide perovskite nanoparticles synthesized with porous alumina media," *Chemistry Letters,* vol. 41, pp. 397-399, 2012.
3. J. H. Im, C. R. Lee, J. W. Lee, S. W. Park, and N. G. Park, "6.5% efficient perovskite quantum-dot-sensitized solar cell," *Nanoscale*, vol. 3, pp. 4088-4093, 2011.
4. M. M. Lee, J. Teuscher, T. Miyasaka, T. N. Murakami, and H. J. Snaith, "Efficient hybrid solar cells based on meso-superstructured organometal halide perovskites," *Science,* vol. 338, pp. 643-647, 2012.
5. R. F. Service, "Cesium fortifies next-generation solar cells," *Science*, vol. 351, pp. 113, 2016.
6. N. K. Kumawat, A. Dey , A. Kumar, S. P. Gopinathan, K. L. Narasimhan, and D. Kabra, "Band Gap Tuning of $CH_3NH_3Pb(Br_{1-x}Cl_x)_3$ Hybrid Perovskite for Blue Electroluminescence," *Appl. Mater. Interfaces,* vol. 7, pp.13119–13124, 2015.
7. T. Baikie, Y. N. Fang, J. M. Kadro, M. Schreyer, F. X. Wei, S. G. Mhaisalkar, M. Graetzel, and T. J. White, "Synthesis and Crystal Chemistry of the Hybrid Perovskite $(CH_3NH_3)PbI_3$ for Solid-State Sensitised Solar Cell Applications," *J Mater Chem A*, vol. 1, pp. 5628−5641, 2013.
8. A. Binek, F. C. Hanusch, P. Docampo, and T. Bein, "Stabilization of the Trigonal High-Temperature Phase of Formamidinium Lead Iodide," *J Phys Chem Lett*, vol. 6, pp.1249-1253, 2015.
9. M. Ye, X. Wen , M. Wang, J. Iocozzia, N. Zhang, C. Lin, and Z. Lin, "Recent advances in dye-sensitized solar cells: from photoanodes, sensitizers and electrolytes to counter electrodes," *Mater Today*, vol. 18, pp.155-162, 2014.
10. M. A. Loi and J. C. Hummelen, "Hybrid solar cells: Perovskites under the Sun," *Nature Mater*, vol. 12, pp. 1087–1089, 2013.
11. I. Deretzis, A. Alberti, G. Pellegrino, E. Smecca, F. Giannazzo, N. Sakai, T. Miyasaka, and A. L. Magna, "Atomistic origins of CH3NH3PbI3 degradation to PbI2 in vacuum," *Appl Phys Lett,* vol. 106, pp. 131904, 2015.
12. A. Amat, E. Mosconi, E. Ronca, C. Quarti, P. Umari, M. K. Nazeeruddin, M. Gratzel, and F. D. Angelis, " Cation-Induced Band-Gap Tuning in Organohalide Perovskites: Interplay of Spin−Orbit Coupling and Octahedra Tilting," *Nano Lett*, vol. 14, pp. 3608-3616, 2014.
13. E. Smecca, Y. Numata, I. Deretzis, G. Pellegrino, S. Boninelli, T. Miyasaka, A. L. Magnaa, and A. Alberti, "Stability of solution-processed MAPbI3 and FAPbI3 layers," *Phys Chem Chem Phys,* vol. 18, pp. 13413-13422, 2016.
14. J. Seo, J. H. Noh, and S. I. Seok, "Rational Strategies for Efficient Perovskite Solar Cells," *Accounts of chemical research,* vol. 49, pp. 562-572, 2016.
15. G. Giorgi, J. I. Fujisawa, H. Segawa, and K. Yamashita, "Cation Role in Structural and Electronic Properties of 3D Organic–Inorganic Halide Perovskites: A DFT Analysis," J *Phys Chem C*, vol. 118, pp. 12176-12183, 2014.
16. W. Setyawan and S. Curtarolo, "High-throughput electronic band structure calculations: Challenges and tools," *Computational Materials Science*, vol. 49, pp. 299-312, 2010.
17. A. A. Zhumekenov, M. I. Saidaminov, M. A. Haque, E. Alarousu, S. P. Sarmah, B. Murali, I. Dursun, X. H. Miao, A. L. Abdelhady, and T. Wu, "Formamidinium Lead Halide Perovskite Crystals with Unprecedented Long Carrier Dynamics and Diffusion Length," *ACS Energy Letters,* vol. 1, pp. 32-37, 2016.
18. W. S. Yang, J. H. Noh, N. J. Jeon, Y. C. Kim, S. Ryu, J. Seo, and S. I. Seok, "A High-performance photovoltaic perovskite layers fabricated through intramolecular exchange," *Science*, vol. 348, pp.1234-1237, 2015.
19. F. Brivio, K. T. Butler, A. Walsh, and M. V. Schilfgaarde, "Relativistic quasiparticle self-consistent electronic structure of hybrid halide perovskite photovoltaic absorbers," *Physical Review B*, vol. 89, pp.155204, 2014.
20. P. Umari, E. Mosconi, and F. D. Angelis, "Relativistic GW calculations on $CH_3NH_3PbI_3$ and $CH_3NH_3SnI_3$ perovskites for solar cell applications," *Scientific reports*, vol. 4, pp. 4467, 2014.
21. Y. Y. Pan, Y. H. Su, C. H. Hsu, L. W. Huang, and C. C. Kaun, "The Electronic Structure of Organic-Inorganic Hybrid Perovskite Solar Cell: A First-Principles Analysis," *Comput Mater Sci,* vol. 117, pp. 573-578, 2016.

